Laser gain measurements by means of amplified spontaneous emission

G. Marowsky, F. K. Tittel, W. L. Wilson, and E. Frenkel

Laser gain determination by means of amplified spontaneous emission is discussed in terms of a rate-equation approach. Numerical solutions show that optical gain can be deduced only for a limited regime of experimental parameters. The theoretical analysis is examined with experimental gain data for organic dyes in the vapor phase and in liquid solution. In addition, the gain of electron-beam-excited Ar–N_2 and XeF laser mixtures has been studied.

I. Introduction

Optical gain is an essential parameter for the characterization of any laser system. Laser threshold conditions, output coupling of the resonator, power output, efficiency, saturation behavior, and spectral narrowing effects are all functions of the gain characteristics of an active medium. The most direct method for measuring optical gain utilizes a laser probe beam of the appropriate wavelength, but frequently no such source exists or is available conveniently, in which case an indirect technique based on the analysis of amplified spontaneous emission (ASE) can be employed.[1] ASE techniques have been used by several groups[2–4] to compare the gain characteristics of organic dyes in liquid solution. Initial analysis of ASE was based on an intuitive approach[2] and subsequently improved by means of a rate-equation approach.[5] In this paper, a detailed computer analysis of the ASE technique is described that utilizes realistic values of typical experimental parameters. Although the model is developed primarily based on the well-known features of the dye laser gain, the ASE technique can be effectively applied to other laser systems. The theoretical analysis establishes well-defined experimental limits of applicability of the ASE techniques that are determined by the stimulated emission cross sections, concentration of active molecules, pump intensity, and geometrical effects. Finally, this analysis is examined in terms of actual experimental gain data for optically and electrically excited organic dyes in liquid solution and in the vapor phase and electron-beam-excited Ar–N_2 and XeF laser mixtures. In the case of organic dyes, the small-signal gain as derived from ASE measurements leads to a determination of the spectral dependence of the excited-state absorption (ESA) cross sections.

II. Theoretical Model

Experimental details of the ASE technique for measuring gain have been described in Refs. 2–5. The technique involves a comparison of the fluorescence yields of various lengths of the active medium. An analysis of this technique can be made in terms of coupled differential laser rate equations that describe the properties of two oppositely traveling waves $I^+(x)$ and $I^-(x)$ [Fig. 1(a)] in a transversely excited active medium. For simplicity, let us consider an ideal four-level system, such as an organic dye of concentration N (total number of molecules/cm^3), excited-state population density N_1, cross section for stimulated emission σ_e, cross section for pump light σ_{ap}^0, absorption cross section for reabsorption σ_{al}^0, and cross section for excited-state absorption of fluorescence radiation σ_{al}^1. The propagation of the ASE intensities $I^+(x)$ and $I^-(x)$ with uniform transverse excitation with a pump intensity I_p may be described by the following equations under stationary conditions[6]:

$$\pm\frac{1}{\sigma_e N}\cdot\frac{d}{dx}I^{\pm}(x) = [g^{\pm}(x) + I^{\pm}(x)(1 + k_l^0 - k_l^1)]\frac{N_1}{N} - k_l^0 I^{\pm}(x), \quad (1)$$

$$N_1(x) = N\cdot\frac{I_p + k_l^0 I(x)}{1 + I_p + \epsilon(1 + k_l^0)I(x)}, \quad (2)$$

$$I(x) = I^+(x) + I^-(x) \quad (3)$$

Equations (1)–(3) have been formulated using dimensionless quantities, and the notation used is the same as in Ref. 5. The intensities I, I^+, I^-, and I_p have been normalized to their saturation intensities, $I_s = (\tau_1\sigma_e)^{-1}$

G. Marowsky is with Max-Planck-Institut fuer Biophysikalische Chemie, Gottingen, Federal Republic of Germany, and E. Frenkel is with Fachhochschule Furtwangen, Furtwangen, Federal Republic of Germany. The other authors are with Rice University, Electrical Engineering Department, Houston, Texas 77001.

Received 7 September 1979.
0003-6935/80/010138-06$00.50/0.

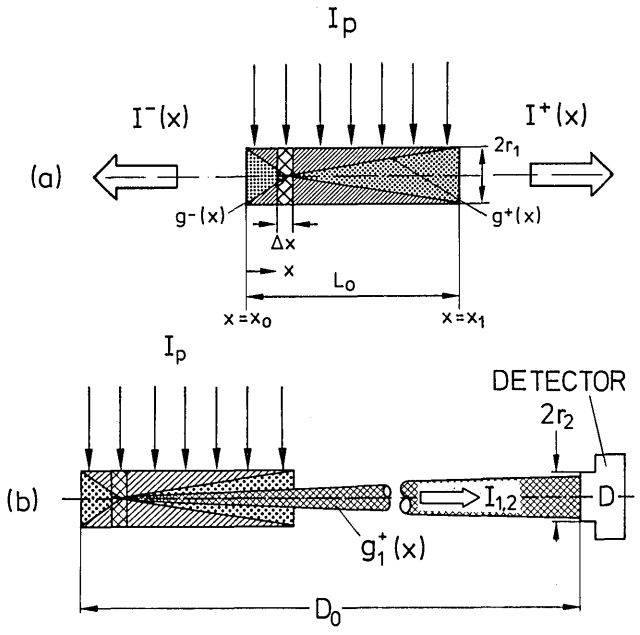

Fig. 1. (a) Transverse excitation scheme for generation of the ASE intensities $I^+(x)$ and $I^-(x)$ and definition of the geometrical factors $g^+(x)$ and $g^-(x)$. (b) Registration of integrated fluorescence intensity $I_{1,2}$ by a detector at a distance $D \gg L_0$.

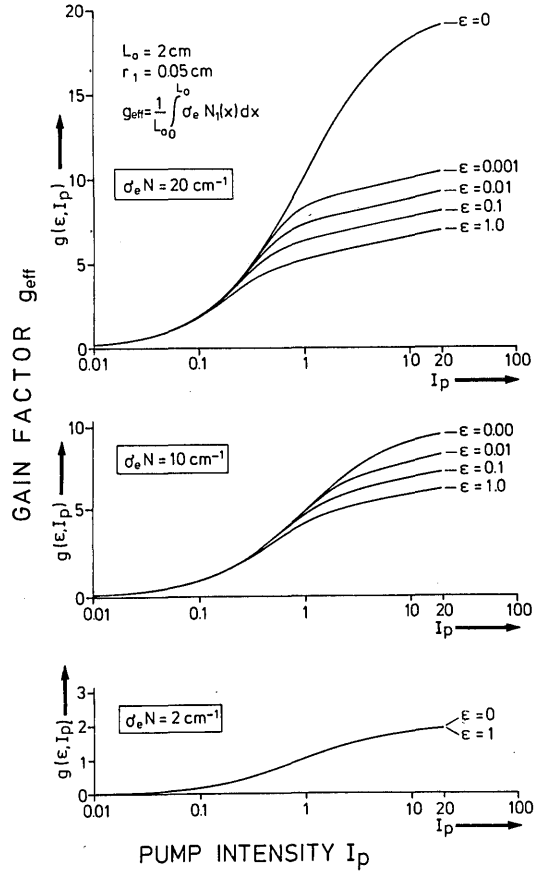

Fig. 2. Computer evaluation of $g(\epsilon, I_p)$ for three different values of the experimental gain parameter $\sigma_e N$.

for the ASE intensities and $I_{ps} = (\tau_1 \sigma_{ap}^0)^{-1}$ for the pump intensity, where τ_1 is the first excited-singlet-state decay time. The coefficients k_1^0 and k_1^1 have been introduced to account for losses due to reabsorption ($k_1^0 \equiv \sigma_{al}^0/\sigma_e$) and losses due to excited-state absorption ($k_1^1 \equiv \sigma_{al}^1/\sigma_e$). The factors $g^{\pm}(x)$ denote the probability that a spontaneously emitted light quantum at point x of the active volume penetrates through the end faces of a cylinder of radius $2r_1$ and length L_0. According to Refs. 5 and 6, these factors are given by

$$g^+(x) = \frac{1}{2}\left\{1 - \frac{L_0 - x}{[(L_0 - x)^2 + r_1^2]^{1/2}}\right\}, \tag{4}$$

$$g^-(x) = \frac{1}{2}\left[1 - \frac{x}{(x^2 + r_1^2)^{1/2}}\right]. \tag{5}$$

The factor ϵ in Eq. (2) describes the reduction of the inversion level due to the influence of ASE. For $\epsilon = 0$, the excited-state depletion by ASE is neglected. For $\epsilon = 0$, $k_l^0 I \ll I_p$, and by neglecting the spatial dependence of $g^{\pm}(x)$, the small-signal gain coefficient g_0 can be derived from Eqs. (1)–(3) upon integration:

$$\begin{aligned} g_0 &= \sigma_e N[I_p(1 - k_l^1) - k_l^0]/(1 + I_p) \\ &= \sigma_e N I_p^*/(1 + I_p) \end{aligned} \tag{6}$$

with

$$I_p^* \equiv I_p(1 - k_l^1) - k_l^0. \tag{6a}$$

On the other hand, a probe beam will experience an effective gain g_{eff}, which can also be derived from the rate equations, taking into consideration their spatial dependence with $g^{\pm} = g^{\pm}(x)$ and $\epsilon = 1$. Then g_{eff} is given by

$$g_{\text{eff}} = \frac{1}{L_0}\int_0^{L_0} \sigma_e N_1(x)dx. \tag{7}$$

The dependence of g_{eff} on the pump intensity I_p is shown in Fig. 2. The plots are obtained from a computer solution of Eqs. (1)–(3) for different values of $\sigma_e N = 2$, 10, and 20 cm^{-1} and different ϵ values. It is apparent from Fig. 2 that for small pump intensities I_p and small $\sigma_e N$ values solutions with $\epsilon = 0$ and $\epsilon = 1$ coincide, and hence $N_1 \neq N_1(x)$ or g_0 as defined in Eq. (6) is a good approximation for the small-signal gain. A value of $\sigma_e N = 10$ cm^{-1} approximately corresponds to the characteristics of a 10^{-4} M solution of an organic dye with a cross section for stimulated emission of 10^{-16} cm^2. For even more dilute solutions ($N \approx 5 \cdot 10^{-5}$ M) and I_p as high as unity, the differences between the approximate solution $g(\epsilon = 0, I_p)$ and the realistic case $g(\epsilon = 1, I_p)$ disappear completely. In the case of a broadband dye laser, it is not necessary to use wavelength-integrated cross sections, as discussed in Ref. 5, and to introduce $g^{\pm}$ factors weighted by the quantum efficiency of the total fluorescence spectrum as long as I_p and $\sigma_e N$ are restricted to the values shown in Fig. 2.

Application of the ASE technique requires alternate exposures of different volumes of the active medium to the pump. According to Ref. 1, the small-signal gain is obtained from the ratio of the resultant amplified spontaneous emissions:

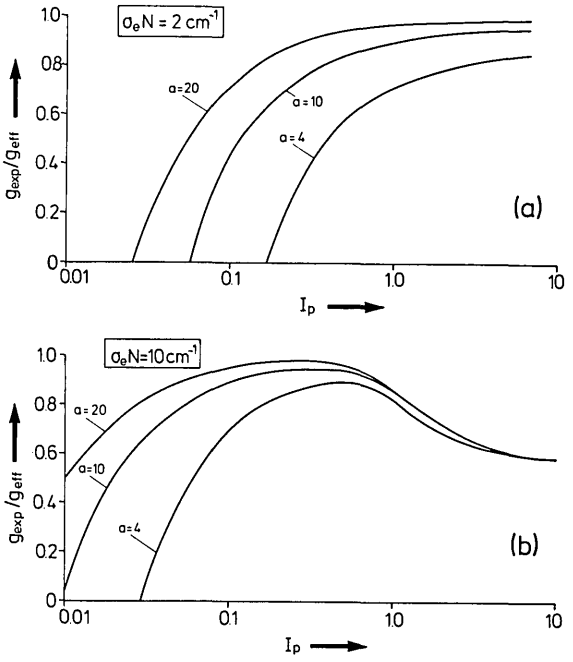

Fig. 3. Comparison of g_{exp} and g_{eff} for (a) $\sigma_e N = 2\ cm^{-1}$ and (b) $\sigma_e N = 10\ cm^{-1}$ for values of $a = 4$, 10, and 20 where $a = D/L_0$.

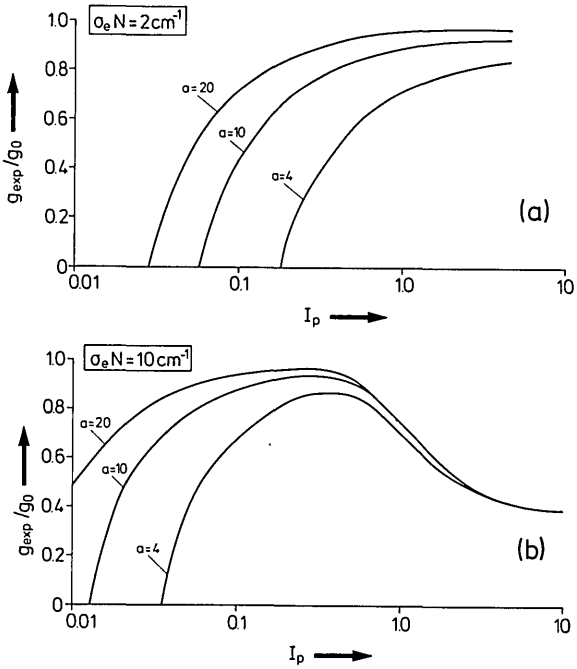

Fig. 4. Comparison of g_{exp} and g_0 for (a) $\sigma_e N = 2\ cm^{-1}$ and (b) $\sigma_e N = 10\ cm^{-1}$ for values of $a = 4$, 10, and 20.

$$g_{exp} = \frac{1}{L_0} \ln \left[\frac{I_2^+(L_0)}{I_1^+\left(\frac{L_0}{2}\right)} - 1 \right]. \tag{8}$$

L_0 is the full length of the pumped region, and $I_2^+(L_0)$ and $I_1^+(L_0/2)$ are the ASE intensities after exposure to the full length L_0 and the half length $L_0/2$. These intensities are monitored with a detector of an entrance-aperture diameter $2r_2$ located at a distance D from the active volume [Fig. 1(b)]. The intensities $I_1^+(L_0/2)$ and $I_2^+(L_0)$ have been obtained by another integration of Eq. (1) with $N_1(x)$ determined by integration with respect to $I^+(x)$ and $I^-(x)$. In the second integration, $g^+(x)$ is given by

$$g_1^+(x) = \frac{1}{2}\left\{1 - \frac{D - x}{[(D-x)^2 + r_2^2]^{1/2}}\right\}. \tag{9}$$

For $k_l^0 = k_l^1 = 0$ and $r_1 = r_2$ we have studied the effect of a geometry factor $a = D/L_0$ on the experimentally determined gain data g_{exp} with respect to g_0 and g_{eff} by a plot of g_{exp}/g_{eff} or g_{exp}/g_0 vs pump intensity I_p. Figures 3 and 4 show the theoretical results for selected values of a and $\sigma_e \cdot N$. The analysis is based on the formulation of the ASE problem by Ganiel *et al.*[6] The model assumes that spontaneous emission at a rate N_1/τ_1 is considered to create stimulated fluorescence only toward the end faces of the active medium within the cones described by $g^+(x)$ and $g^-(x)$. According to Figs. 3 and 4, the experimentally determined gain data g_{exp} are close to the effective gain g_{eff} and g_0 only for restricted ranges of the geometry factor a. For low $\sigma_e N$ values, it can be deduced from Figs. 3(a) and 4(a) that a minimum detector distance $D \geq 20L_0$ is required and that the pump power must be close to unity or greater in order to assure independence of gain data from detector position. On the other hand, g_{exp}/g_{eff} and g_{exp}/g_0 values deviate considerably from unity if I_p exceeds unity and $\sigma_e N \geq 2\ cm^{-1}$ [Figs. 3(b) and 4(b)]. As a consequence, low $\sigma_e N$ values, I_p values close to 1, and a detector position $D \gg L_0$ should be chosen for a reliable gain measurement when using the ASE technique. As shown in Figs. 3(b) and 4(b), only in this range of experimental values is it justified to approximate g_{eff} with g_0, a necessary step for a further evaluation of $g_0 = g_0(k_l^0, k_l^1, \ldots)$. On the other hand, Figs. 3 and 4 show that the experimentally determined gain figures g_{exp} are always $< g_0$ and g_{eff} or that the actual gain always exceeds the gain measured by the ASE technique, even in the absence of gain saturation.

III. Experimental

A comparison of fluorescence from various pumped lengths of a laser medium can be achieved by different experimental methods.[4,7] Figure 5(a) depicts the details of a method that compares two pumped lengths $L_0/2$ and L_0 of an active medium, while Fig. 5(b) shows a procedure that evaluates the fluorescence signals produced upon exposure of length L_0 or $2L_0$ to the pump beam by means of a partial reflector. The latter technique allows simultaneous registration of both a transmitted signal $I_1(L_0)$ and a reflected signal $I_2(2L_0)$. Thus this method eliminates shot-to-shot fluctuations for the low repetition rate of such excitation sources as a high-power electron beam accelerator. In addition, probing the entire excited volume minimizes any in-

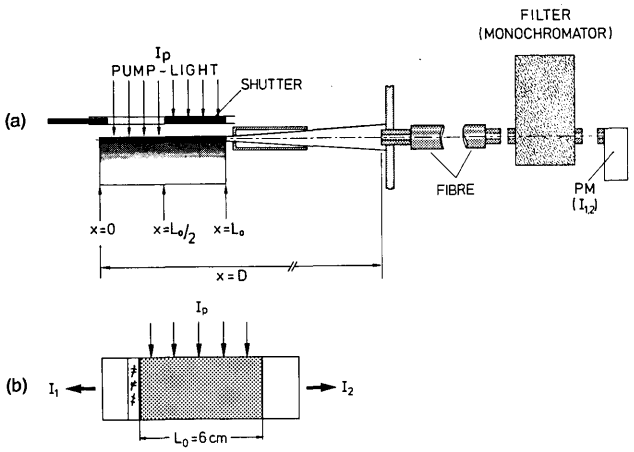

Fig. 5. (a) Experimental setup for gain measurement using the ASE technique by comparing different pumped lengths of the active medium. (b) Schematic of ASE gain determination using an internal mirror for a comparison of the intensities $I_1 = I(L_0)$ and $I_2 = I(2L_0)$.

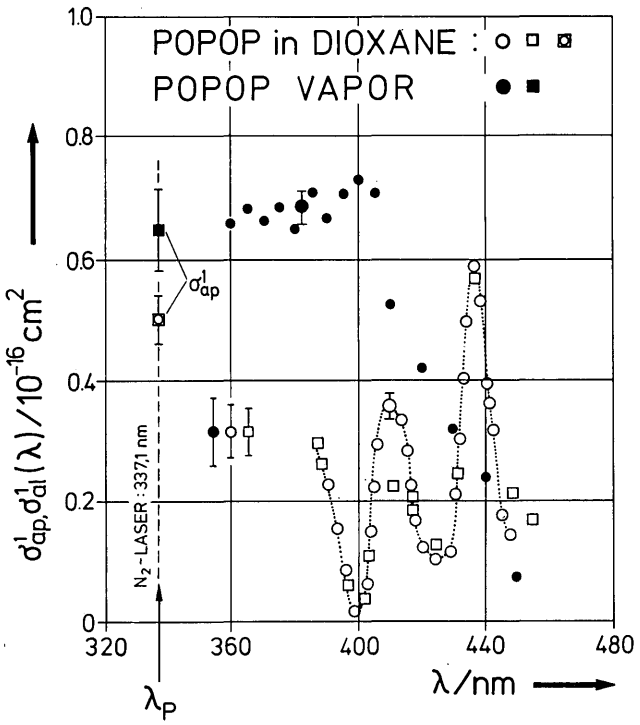

Fig. 7. Spectral dependence of excited-state cross sections for POPOP in the vapor phase (●) and in liquid solution (○, □). σ^1_{ap} denotes excited-state absorption cross section of a N_2 laser pump.

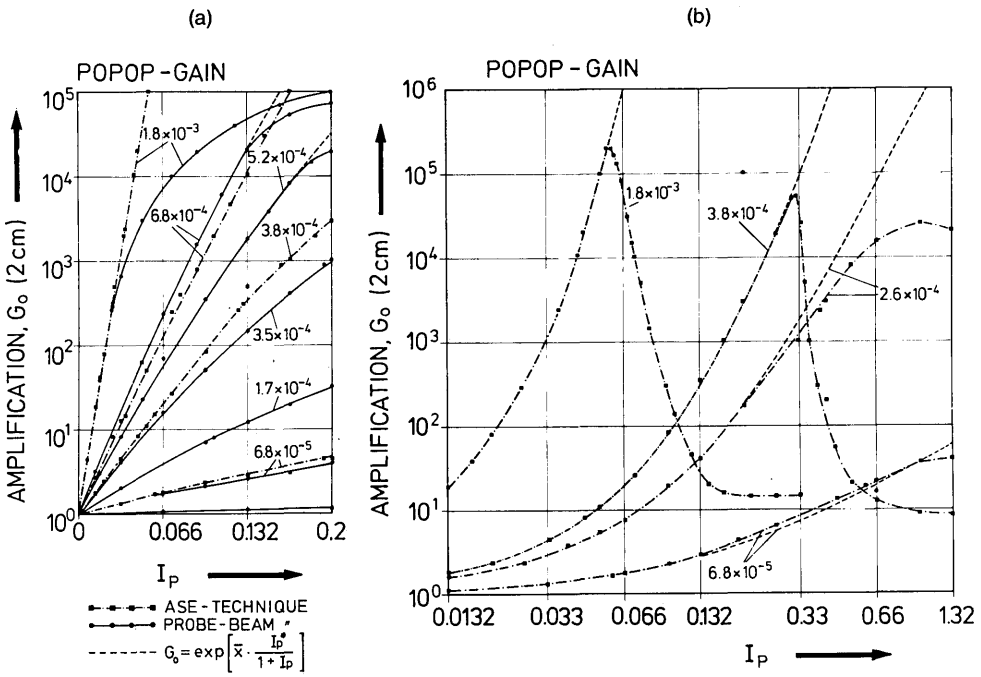

Fig. 6. Experimental comparison of gain measurements using the ASE technique and the laser probe beam for different concentrations of the dye POPOP in a dioxane solution for (a) $I_p \leq 0.2$ and (b) $I_p \leq 1.3$. The ASE data agree with the small-signal gain approximation $G_0 = \exp[\bar{x} \cdot I_p^*/(1 + I_p)]$, where $\bar{x} = N \cdot \sigma_e \cdot L_0$ and I_p^* are defined by Eq. (6a).

homogeneities introduced by the excitation source, which may lead to serious errors if sections of nonuniform pumping are compared.

The validity of the ASE model may be checked by comparison of experimental gain data taken for N_2-laser-excited POPOP (*p*-phenylene-*bis*-oxazole) dye in dioxane solution using both a conventional probe beam and the ASE technique described above. Figures 6(a) and (b) show the result of this comparison by means of a plot of total gain $G_0 = \exp(gL_0)$ with $L_0 = 2$ cm and different POPOP concentrations vs pump power intensity. From this plot it is evident that for small concentrations N and σ_e = constant = $1.6 \cdot 10^{-16}$ cm^2,[8] corresponding to a fluorescence peak at 411 nm, no gain saturation appears and the experimental gain law is valid with $g \approx g_0 \approx g_{exp}$. Small-signal gain data can be derived up to higher pump intensities than can data taken with a laser probe beam. This is more clearly shown in Fig. 6(b), where the I_p range is expanded up to 1.3, corresponding to an actual power density of 10 MW/cm^2 at the N_2-laser wavelength of 337.1 nm. The figure shows in addition the breakdown of the ASE method when the system reaches the threshold for superradiant emission. Even close to this threshold, ASE gain data follow the theoretical prediction of the exponential small-signal gain. The threshold for superradiant emission always appeared at critical $G_0^{crit} = \exp(g^{crit}L_0)$, with g^{crit} essentially determined by the parameters included in Eq. (6), which means that $g^{crit} \sim N$ and $g^{crit} \sim I_p/(1 + I_p)$.

Equation (6) for g_0 allows an evaluation of the dependence of $g_0(I_p)$ with respect to other unknown laser gain parameters such as absorption of the fluorescence radiation by excited states. Figure 7 shows the experimental results of a study of excited-state absorption of POPOP dye in liquid solution and in the vapor phase. The spectral dependence of excited cross sections σ_{al}^1 is plotted in this figure. Two additional points show the ESA cross sections of POPOP at the pump wavelength of 337.1 nm.[9] Values of $\sigma_{al}^1 = 0.6 \cdot 10^{-16}$ cm^2 for POPOP in solution and $\sigma_{al}^1 = 0.7 \cdot 10^{-16}$ cm^2 for POPOP vapor can be derived from Fig. 8 for the two fluorescence peaks centered at 411 nm and 382 nm, respectively. Part of the data for POPOP in solution has been confirmed by means of a laser probe beam source of appropriate wavelength, indicating that good agreement exists with data taken using the ASE technique.

A small-signal gain of 0.25 cm^{-1} has been measured for electron-beam-excited mixtures of POPOP vapor and high-purity argon as buffer gas[9] using the mirror technique. Electron-beam excitation was accomplished with a Physics International Pulserad model 110 accelerator that provided a 20-kA pump pulse of 10-nsec duration at 1 MeV. Current densities up to 1 kA/cm^2 were measured with a Faraday cup probe placed inside the laser cell. In Fig. 8(a) calibration of the no-gain–no-loss situation is displayed with the signal $I_2(2L_0)$ electrically delayed by 60 nsec. The lower trace [Fig. 8(b)] displays the fluorescence intensity at higher argon pressure for which optical gain is present. The internal-mirror ASE method has also been applied to

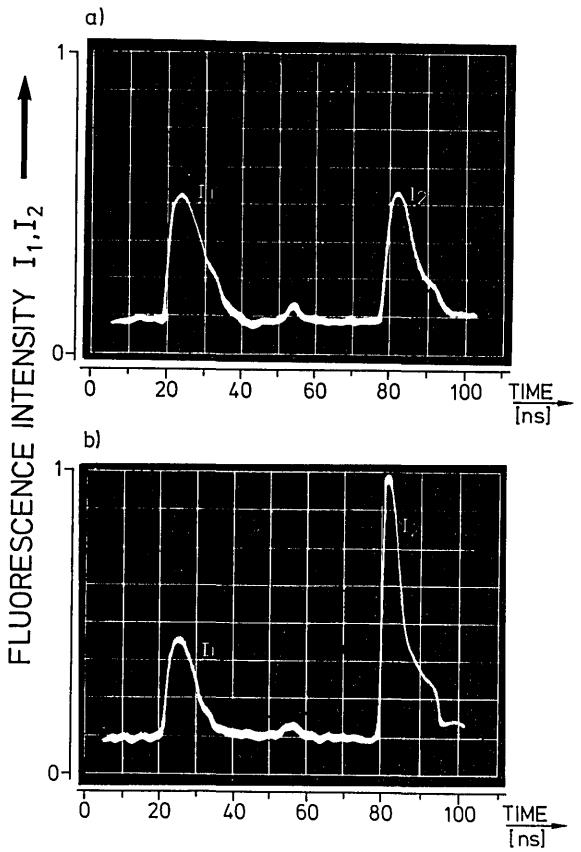

Fig. 8. ASE gain data for electron-beam excited mixtures of POPOP vapor and high-purity argon (for details see Ref. 9). (a) Calibration: no-gain–no-loss (3 atm Ar). (b) $I_2/I_1 = 2.6$, $\alpha_{net} = 25\%$ cm^{-1} (4.5 atm Ar).

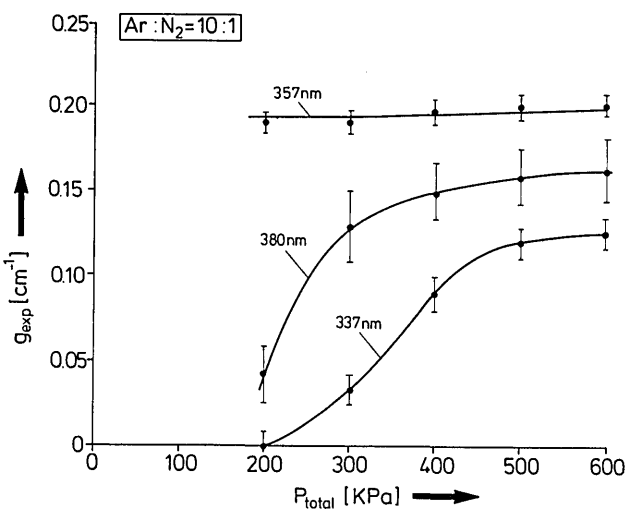

Fig. 9. Dependence of argon buffer pressure of gain of the individual N_2 transitions at 337, 357, and 380 μm and integrated total gain for the Ar–N_2 laser.

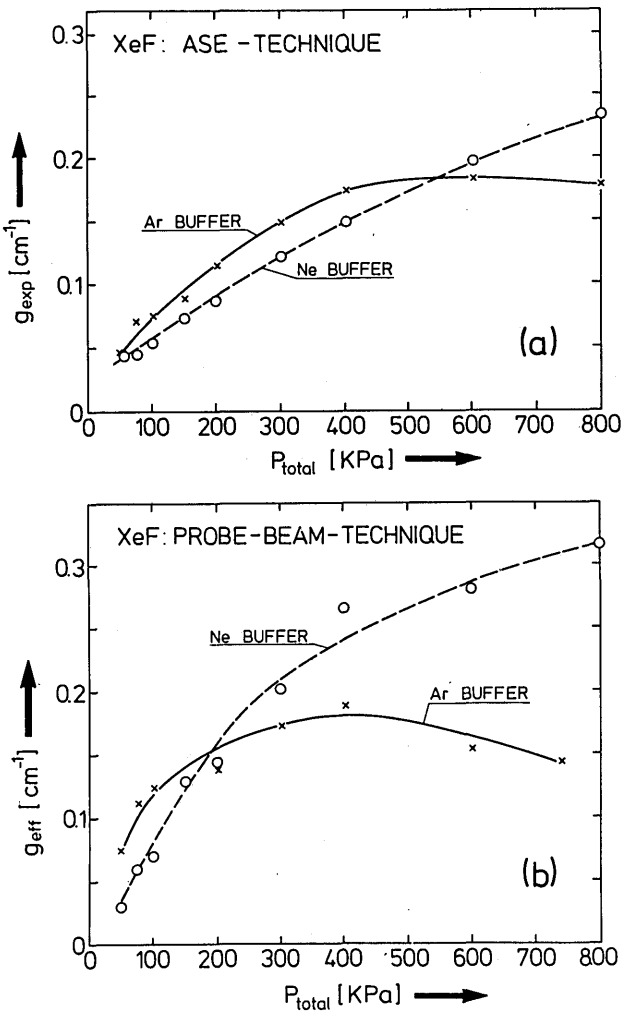

Fig. 10. Gain of electron-beam excited XeF laser mixtures vs pressure of Ar and Ne buffer gas pressure using (a) the ASE technique and (b) cw argon-ion laser probe beam at 351 nm. All data were obtained with 16-Torr Xe and 8-Torr NF_3 partial pressures.

studying the gain characteristics and kinetic processes of electron-beam-excited Ar–N_2 laser mixtures.[10,11] Figure 9 shows the good agreement between the wavelength-integrated gain and the appropriately weighted contributions of the gain of the individual lines at 337, 357, and 380 nm in a plot of g_{exp} vs total pressure for a standard 10:1 mixture of argon and nitrogen. Partial gain saturation, especially at high pressure, cannot be excluded, but it is difficult to estimate the appropriate σ_e–N–I_p range of the Ar–N_2 laser system.

Further laser gain measurements have been made of electron-beam-pumped XeF laser mixtures at 351 nm.[12] Figure 10 shows the pressure dependence of the small-signal gain at peak intensity for an argon or neon buffer gas mixture. Figure 10(a) depicts gain data obtained by the ASE-mirror technique, which in Fig. 10(b) are compared with gain data obtained directly using a 351-nm argon-ion laser probe beam. The higher optical gain figures observed with neon buffer gas are due to less buffer gas absorption than for argon.[13] In fact, the different results for the two experimental methods were in agreement with theoretical predictions. The gain probed with the argon laser beam should be close to g_{eff} and should be higher than the data obtained by the ASE method. In principle, a comparison of the data obtained by both methods should allow an estimate of the effective saturation power density I_p in the case of electron-beam excitation. The quantity I_p is more readily available in optical excitation experiments with well-defined cross sections for absorption of the pump radiation.

IV. Discussion

The reliability and versatility of probing laser gain using ASE techniques has been illustrated by several examples. The experimental restrictions such as positioning of the fluorescence detector far from the excited volume can be fulfilled without experiencing low SNRs due to the $1/r^2$ dependence of the fluorescence radiation. Excited-state cross sections can be deduced from ASE data, which directly yield small-signal gain. In contrast, a technique using the laser probe beam gain requires the existence of a tunable or wavelength-matched coherent light source in the spectral range of interest in order to probe the fluorescence profile. If a pulsed probe is used, careful synchronization between the pulsed excitation source, such as an electron-beam accelerator, and the pulsed laser source must be achieved.[14] The best agreement between experimental gain data g_{exp} for an organic dye laser obtained by the ASE technique and the effective gain g_{eff} is at low dye concentrations (N) and relative high pumping powers (I_p) when the data are taken in the far-field distribution of the transverse-excited stimulated fluorescence. Furthermore, the numerical analysis used is based on stationary solutions of the rate equations, which can be assumed to be valid in the case of e-beam excited organic dyes (with $\tau_1 \approx 1$ nsec) but is not correct for the Ar–N_2 and XeF laser systems.

This work was supported by the Office of Naval Research, the Robert A. Welch Foundation, and the National Science Foundation.

References

1. W. T. Silfvast and J. S. Deech, Appl. Phys. Lett. **11**, 94 (1967).
2. P. W. Smith, P. F. Liao, C. V. Shank, C. Lin, and P. J. Maloney, IEEE J. Quantum Electron. **QE-11**, 84 (1975).
3. C. V. Shank, Rev. Mod. Phys. **47**, 649 (1975).
4. A. Dienes, C. V. Shank, and R. L. Kohn, IEEE J. Quantum Electron. **QE-9**, 833 (1973).
5. W. Heudorfer, G. Marowsky, and F. K. Tittel, Z. Naturforsch. **33a**, 1062 (1978).
6. U. Ganiel, A. Hardy, G. Neumann, and D. Treves, IEEE J. Quantum Electron. **QE-11**, 881 (1975).
7. A. W. Johnson and J. B. Gerardo, J. Appl. Phys. **46**, 4870 (1975).
8. B. Steyer and F. P. Schaefer, Appl. Phys. **7**, 113 (1975).
9. G. Marowsky, IEEE J. Quantum Electron. **16**, (Jan. 1980).
10. M. L. Bhaumik, Inst. Phys. Conf. Ser. **29**, 122 (1976).
11. W. E. Ernst, F. K. Tittel, W. L. Wilson, and G. Marowsky, J. Appl. Phys. **50**, 3879 (1979).
12. W. E. Ernst, C. Pollock, F. K. Tittel, and W. L. Wilson, to be published.
13. E. Zamir, D. L. Huestis, H. H. Nakoma, R. M. Hill, and D. C. Lorents, IEEE J. Quantum Electron. **QE-15**, 281 (1978).
14. A. M. Hawrylnk, J. A. Mangano, and J. H. Jacob, Appl. Phys. Lett. **31**, 164 (1977).